



IR challenges and the machine detector interface at FCC-ee

Manuela Boscolo^{1,2,a} , Helmut Burkhardt², Katsunobu Oide³ ,
Michael K. Sullivan⁴

¹ INFN, Frascati, Italy

² CERN, Meyrin, Switzerland

³ KEK, Tsukuba, Japan

⁴ SLAC, Menlo Park, USA

Received: 16 April 2021 / Accepted: 3 October 2021

© The Author(s) 2021

Abstract The FCC-ee, with its unprecedented luminosity goal and high energy reach, creates challenges and requires solutions to many issues in order to produce a realistic design for the complex machine detector interface. The interaction region design for the FCC-ee adopts the crab-waist collision scheme and proposes an elegant local chromaticity correction system. An asymmetric layout of nearby dipoles suppresses the critical energy of synchrotron radiation incoming to the detector at the interaction point to a maximum value of 100 keV. The main challenge of the FCC-ee machine detector interface design is to combine the many conflicting accelerator and 2 T detector constraints, aiming for the optimal trade-off choices that simultaneously allow for a best machine performance in terms of integrated luminosity and data taking efficiency. Much of the success of the FCC-ee will be related to the interaction region design, as a result of the ingredients coming from areas of accelerator physics, mechanical engineering and detector optimization.

1 Introduction

The Future Circular Collider (FCC-ee) [1] aims to make precision studies and rare decay observations in the range of 90 to 365 GeV centre-of-mass energy. This energy range will allow precision measurements of the Z and W bosons with unique accuracy as well as exploring the high energy frontier up to the Higgs boson and top quark. The unprecedented ring circumference of ~ 100 km allows for a target luminosity per IP of $2 \times 10^{36} \text{ cm}^{-2} \text{ s}^{-1}$ at the Z pole and the ability to reach the $t\bar{t}$ energy with $1.8 \times 10^{34} \text{ cm}^{-2} \text{ s}^{-1}$ luminosity. The Z pole run will be characterized by the demand for high luminosity, requiring a high beam intensity operation mode. The top energy will be at low beam intensity to mitigate the beam emitted synchrotron radiation. All the different energy stages are characterized by the same radiation beam power, set to 50 MW per beam. The high intensity and high energy

M. K. Sullivan: This material is based on work supported by the US Department of Energy, Office of Science, under Contract No. DE-AC02-76SF-00515.

This work was partially supported by the EC HORIZON 2020 project FCC-IS, Grant agreement n.951754.

^a e-mail: Manuela.boscolo@Inf.infn.it (corresponding author)

operation modes have an immediate impact on the interaction region (IR) optics as well as on the machine detector interface (MDI) design that is unique for all running energies.

The paper is organized as follows. We describe the IR optics in Sect. 2, the IR layout with challenges for the mechanical engineering design in Sect. 3, and the beam backgrounds in Sect. 4. While pointing out the challenges for the different aspects of this design, we also discuss the ongoing work and our plan for further studies.

2 Optics design in the IR

The baseline beam optics was established in 2016 [2], then further revised in [3,4]. The optics scales with the energy allowing for a common IR layout at all energies. The crab-waist collision scheme [5] has been chosen for the interaction region design. Two IPs are foreseen in the baseline, the option of having 4 IPs is presently under study, especially with regard to establishing the tune footprint, to consider the beam-beam effect with realistic orbit errors, and also to evaluate the possible luminosity reduction per IP. Table 1 lists the most relevant beam parameters for the IR and MDI studies.

One of the beam optics challenges for the collider is to provide an adequate dynamic aperture with small β -functions at the interaction point down to $\beta_x = 0.15$ m and $\beta_y = 0.8$ mm at the Z pole.

These values, together with an ℓ^* of 2.2 m, the distance between the face of the final quadrupole magnet to the IP, produce a vertical chromaticity around the IP as high as in modern B factories that is corrected locally. At the $t\bar{t}$ energy, a very wide momentum acceptance is required due to the beamstrahlung caused by the collisions. The transverse on-momentum dynamical aperture must be larger than $\sim 12\sigma_x$ to enable top-up injection in the horizontal plane.

The beam lines in the interaction region are separated for the two beams and there are no common quadrupoles in the IR. The full horizontal crossing angle is 30 mrad. The detector solenoid is 2 T and its effect on the stored beams is compensated with anti-solenoids, which cancel the $\int B_z dz$ between the IP and the faces of the final quadrupole [6]. The vertical emittance increases due to the fringe field of the compensating solenoid combined with the horizontal crossing angle. However, the increase in the vertical emittance is estimated to remain below 0.3 pm for 2 IPs.

The optimized values of $\beta_{x,y}^*$ are smaller at the lower beam energies. This flexibility is obtained by splitting the first quadrupole into three slices and modulating the sign and strength accordingly, with an upper limit of 100 T/m for the field strength.

One of the main guidelines of the IR design has been to keep the critical energy of the synchrotron radiation (SR) from bending magnets below 100 keV up to 500 m from the IP for the incoming beam and to have the last upstream dipole located at least 100 m from the IP. This requirement is guided by the LEP2 experience, where manageable detector backgrounds were found with a critical energy of 72 keV from 260 m from the IP [7]. The SR from the last bend is described in more detail in Sect. 4.1. An asymmetric optics allows the beam to come from the inner ring to the IP, then bend strongly after the IP to merge back close to the opposing ring, in order to fulfil the critical energy requirement in the presence of a large crossing angle.

Some of the topics needing further study in order to refine the baseline optics in the interaction region are: the implementation of the solenoids in the MAD-X baseline model, in addition to the SAD model, the inclusion of the correction windings of the final focus quadrupoles and fringing fields, the modelling of the local chromatic and crab sextupoles,

Table 1 FCC-ee beam parameters most related to IR design

	Z	W	H	$t\bar{t}$
Circumference (km)	97.756	97.756	97.756	97.756
Crossing angle at IP (mrad)	30	30	30	30
L^* (m)	2.2	2.2	2.2	2.2
SR power/beam (MW)	50	50	50	50
Beam energy (GeV)	45.6	80	120	182.5
Luminosity/IP ($10^{34}\text{cm}^{-2}\text{s}^{-1}$)	230	28	8.5	1.55
β_x^* (m)	0.15	0.2	0.3	1
β_y^* (mm)	0.8	1	1	1.6
ϵ_x (nm)	0.27	0.84	0.63	1.46
ϵ_y (pm)	1.0	1.7	1.3	2.9
σ_x^* (μm)	6.4	13.0	13.7	38.2
σ_y^* (μm)	28	41	36	68
Beam current (mA)	1390	147	29	5.4
Bunch population (10^{11})	1.7	1.5	1.8	2.3
Bunch number/beam (#)	16640	2000	328	48
Average bunch spacing (ns)	19.6	163	994	3396
Effective length of interaction (mm)	0.42	0.85	0.90	1.8
SR loss/turn (GeV)	0.036	0.34	1.72	9.21
Bunch length by SR /BS (mm)	3.5/12.1	3.0/6.0	3.15/5.3	1.97/2.54
Energy acceptance (%)	1.3	1.3	1.7	$-2.8 + 2.4$

and the modelling of the very long dipoles in the interaction region, as well as those in the arcs, into realistic lengths. Another important aspect of the beam optics related to the MDI design is the collimation scheme, which will be implemented around the ring. The collimation settings will also be optimized to minimize the beam backgrounds in the IR, and collimators upstream of the IR might be necessary to reduce beam losses in the experiment in addition to the ones used for masking the SR. Ongoing work to optimize the engineering infrastructure is looking at the footprint of the FCC-hh and FCC-ee colliders in the IR, with the aim to reduce tunnel construction. One solution under investigation is to move the FCC-hh to match the FCC-ee footprint.

3 Interaction region layout

Figure 1 displays the current interaction region layout in an expanded vertical scale. The face of the final focus magnet (QC1) from the IP, ℓ^* , is 2.2 m. The compensating solenoid for the detector field is located from 1.2 to 2.2 m from the IP on either side and is shown in light green. Just in front of the compensating solenoids is a luminosity calorimeter, shown in magenta in the plot. The superconducting final focus magnets will be surrounded by screening solenoids to cancel the 2 T detector field. The overlap of the solenoid and quadrupole fields are minimized and only appearing at the their fringes.

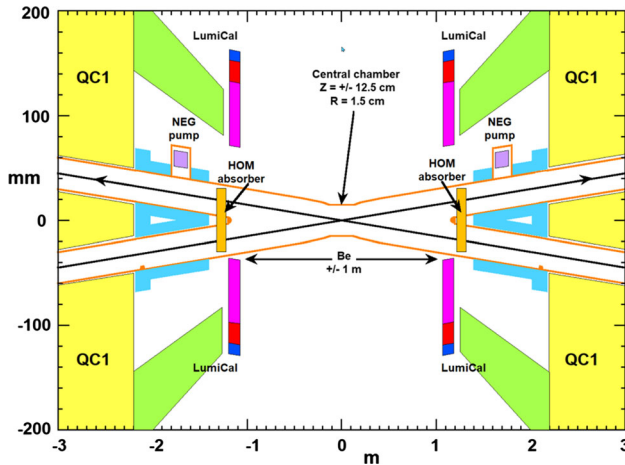


Fig. 1 IR layout. Note the large-scale difference between the vertical and horizontal axes

Two separate circular beam pipes host the two beams and only in the IR are they merged together into a single circular vacuum chamber. The diameter of the central vacuum chamber is 30 mm in the CDR, and the option of reducing it to 20 mm is being considered and investigated. The material of the central part of the beam pipe will be Be to minimize multiple scattering. The impact of the higher-order modes, heat load, and SR has been evaluated for the 30 and 20 mm diameter vacuum chamber. In addition, optimization of the thickness of the SR masks, located on the inner horizontal plane of the incoming beam pipe, has been done for both cases. SR masks are placed after the QC1 upstream of the IP and only on the inner side of the incoming beam (see Fig. 1). Outside the vacuum chamber and surrounding the SR masks, there is a tungsten shielding to protect the detector environment (shown in light blue in Fig. 1).

An engineering mechanical design of the central vacuum chamber, where two vacuum chambers are merged together maintaining a constant aperture, has been used to evaluate electromagnetic fields in the IR. These studies show that for a chamber with a 30-mm diameter, higher-order mode absorbers are necessary. They are positioned just after the luminosity calorimeter (see in Fig. 1 the dark yellow boxes at 1.3 m, where the vacuum chambers split). They have been designed following the experience obtained at the PEP-II B-Facility [8]. A similar study for the smaller diameter vacuum chamber has shown that the trapped higher order modes are significantly reduced, making the absorbers unnecessary. This result is obtained using a model that includes the SR masks located in the inner radial plane that have a gently sloped transition to the beam pipe wall [9].

An overview of the MDI design is found in Refs. [10, 11]. Further, work foreseen to assess the MDI layout is to verify the sustainability of the beam backgrounds and optimizing physical aperture, masks and background shielding accordingly. An engineering design of the IR is necessary in order to integrate magnets, cryostat, IP detectors, vacuum system, supporting structures, and shielding.

4 Optimization of experimental conditions

The FCC-ee is designed as a Higgs factory and as a high precision $e+e-$ collider, covering Z , W and top production. Compared to its predecessor, LEP, the collision energy range is extended by a factor of 1.8, from 207 to 365 GeV in the centre of mass. The FCC-ee target luminosity of $2.3 \times 10^{36} \text{ cm}^{-2}\text{s}^{-1}$ at the Z would be 20,000 times higher than at LEP. In addition to providing very high luminosity, it will also be essential to provide good experimental conditions for the particle detectors installed around the collision regions. Criteria for good experimental conditions are

- Low backgrounds
- Minimizing the risk of damaging sensitive detectors by beam loss and irradiation
- Good stability and knowledge of the beam parameters
- Maximize the space available for the detector.

These are rather conflicting requirements. Minimizing the size of the beam pipe for installation of sensitive vertex detectors close to the beam pipe will increase the background rates hitting the detector region and increase the risk of damage by beam loss. The requirements for maximum space and solid angle coverage for the detectors are also in conflict with the requirements of the accelerator to maximize luminosity by

- Allowing for space close to the interaction point for final focus quadrupoles
- Reducing the β -function at the interaction point, which increases the beam size in the final focus quadrupoles with the risk of creating local aperture limits and losses and which limits the space and low angle coverage available for particle detection
- Installation of beam separators close to the interaction region to allow to fill the machine with many bunches.

We believe that it is essential to consider the accelerator and detector requirements together, both during the design stage described here as well as later in the optimization of the running parameters.

Of particular importance is the simulation of the stored beam halo or non-Gaussian transverse beam tails. These beam particle distributions are generated by several sources, beam-gas collisions, inter-beam bunch scattering, the collision at the IP including Bhabha and radiative Bhabha scattering which are called the luminosity terms, bunch–bunch coupling, and wake-field interaction to name a few. The large number of source terms that put beam particles out into these tail distributions makes it difficult to model these distributions. In the early running of an electron collider, generally, the dominant source terms for the beam tail distributions are from the beam-gas events that occur around the entire ring. Later, when the ring vacuum has improved, other source terms begin to dominate like the luminosity terms as the luminosity improves. The beam tail distribution can be a fairly large fraction (up to a few %) of the core distribution. The combined effects of residual dispersion, coupling and synchrotron radiation emittance around the ring(s) can maintain a high rate of beam tail re-population from the various sources.

We note here that the Z pole, and perhaps the WW energy, of the FCC-ee will be very high-current, low-energy (for the circumference) colliders and in this way much more like the B-factories, while the Higgs and top energy points with significantly lower beam currents and number of bunches and will be much more like the LEP and LEP-II colliders. With this in mind, we must pay close attention to the experience of the B-factories as well as the LEP experience as the design of the FCC-ee IR must include both running conditions.

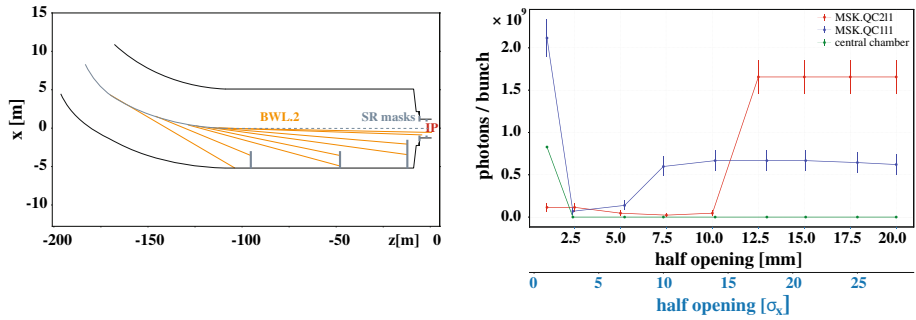


Fig. 2 Synchrotron radiation background and mitigation

Work is currently ongoing and work will continue moving ahead to study the possible beam-tail distributions and to model the effects of the various distributions on detector backgrounds as well as accelerator performance.

4.1 Synchrotron radiation

As described above, the FCC-ee layout has been chosen to reduce the flux of synchrotron radiation towards the experiments. We use detailed simulations to estimate backgrounds by synchrotron radiation and particle losses into the detector region and mitigation by masks and collimators. An efficient SR masking and shielding design used to protect the detectors and produce a sustainable maximum occupancy have been studied and described in the CDR (see also Refs. [12–14]). The possible sources of background from SR come from the last bending magnet from the IP. The radiation fan is minimized by placing the dipole as far as 100 m from the IP. Nevertheless, it is expected to be the dominant source of SR background for the detector. Two mask tips in front of the first final focus quadrupole are placed to intercept these two radiation fans and prevent photons from directly striking the central Be vacuum chamber. Modified version of SYNC_BKG is used to evaluate SR from final focus quads and design the IR with masks and shieldings. This program can study SR from final focus quads that are on axis, and it treats also offset and tilted quads and bend magnets. It includes all relevant cross sections for photon absorption and scattering including specular reflection, which presently is not included in GEANT4 for keV photons at very small scattering angles.

In addition, based on LEP experience, three collimators are placed in each upstream beam pipe to stop the SR fans on surfaces sloped so that they are unable to forward scatter photons towards the IP [15]. Figure 2 shows on the left their longitudinal position, and on the right, the impact on the photon rates depending on the collimator setting. Full GEANT4 studies which include a model of the entire beam pipe and of the nearby sub-detectors of the scattered photons from the mask tips have shown encouraging results. The simulation with a refined model of the vacuum chamber, accelerator components, masks, shielding and collimators is underway also with the aim of providing a flexible tool that can determine the variation of machine backgrounds for different conditions.

The latest studies of SR backgrounds are investigating the possibility of a 20 mm diameter for the central beam pipe, ± 9 cm long at the various running energies. At the Z pole and Higgs energy, the radiation coming from the last bend is blocked by moving the mask tips by 3 mm closer to the beam centreline, while there are some direct hits on the central chamber from the final focus quadrupoles. The photon energies are low at the Z pole which greatly

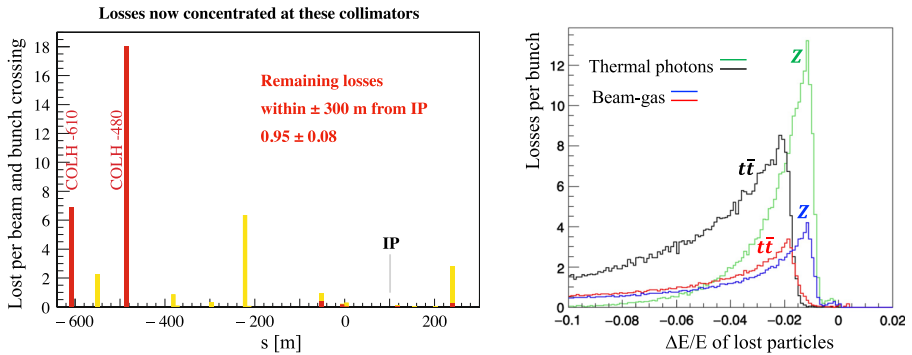


Fig. 3 Off momentum particle losses: loss map from thermal photons with (red) and without (yellow) collimation (left); energy spectrum of lost particles, with 0.001 $\Delta E/E$ per bin (right)

limits the number of photons that can cause detector backgrounds. The relevance of this effect depends on the beam tails, which can vary greatly depending on the stored beam conditions. For the Higgs and the top energy, a careful study with a full GEANT4 simulation and with a realistic beam pipe is needed to evaluate carefully the increase in the SR background in the detector, and to consider the effect of the increased size of the mask tips.

4.2 Beam-induced backgrounds

In addition to our detailed simulations in the IR region, we have also performed tracking studies for the whole ring. Particle tracking using the Monte Carlo technique can evaluate different effects and determine beam losses around the ring. This is a first step towards the design of a collimation scheme and proper setting that will minimize beam losses at the IR.

First results have already been described in the conceptual design report, indicating that backgrounds induced by beam losses in the detector region should be manageable. The studies are continued and refined and checked using different methods. We now also use the element by element transport map information available from MAD-X to track particles for several turns around the ring, with aperture checks performed at element boundaries. Further studies are planned and underway to use a more realistic beam optics model, and to have a fast interface with the corresponding detector backgrounds. Independent MC simulations have been performed for inelastic beam gas [16, 17] and for the thermal photon scattering losses [17, 18] in the MDI area. An example of loss map due to thermal photons including a first proposal for off-momentum collimator positions in the interaction region, and energy spectrum is given in Fig. 3.

Evaluations have been performed with an ideal lattice, showing encouraging results. Systematic further studies are underway including a refined lattice, orbit distortions, chromatic aberrations, radiation damping and energy tapering. These studies together with the modelling of non-Gaussian tails will allow us to evaluate a collimation setting with regard to the backgrounds seen in the detectors.

Particle tracking simulation of beam particles after radiative Bhabha scattering at the Z energy has been performed [19] finding losses at 25 m after the IP and at 400 m. The heat load due to these beam losses bring 150 W within the first final focus quadrupole (QC1) and 400 kW at 400 m. Benchmarking with MADX and GEANT4 simulation of beam losses and photons close to the detector is planned.

The beamstrahlung spent beam particles have been tracked for multiple turns evaluating the beam losses, as well as the photon fans starting from the IP and hitting the vacuum chamber well after the IR, at around 50 m. Direct induced backgrounds in the detector have also been studied. This is a relevant process for FCC-ee, due to its high energy and high intensity. This will require further investigation and dedicated shielding optimization in the downstream part of the beam pipe from the detector.

5 Conclusion

We have described several of the challenges of the FCC-ee MDI layout, discussing the IR optics, parameter choices, physics requirements, and backgrounds, in particular synchrotron radiation. We have also discussed the ongoing and future studies which have been started following the recommendations of the European Particle Physics Strategy Update which are to demonstrate, in the next five years, the feasibility of this collider.

Funding Open Access funding provided by CERN.

Open Access This article is licensed under a Creative Commons Attribution 4.0 International License, which permits use, sharing, adaptation, distribution and reproduction in any medium or format, as long as you give appropriate credit to the original author(s) and the source, provide a link to the Creative Commons licence, and indicate if changes were made. The images or other third party material in this article are included in the article's Creative Commons licence, unless indicated otherwise in a credit line to the material. If material is not included in the article's Creative Commons licence and your intended use is not permitted by statutory regulation or exceeds the permitted use, you will need to obtain permission directly from the copyright holder. To view a copy of this licence, visit <http://creativecommons.org/licenses/by/4.0/>.

References

1. A. Abada et al., FCC. Eur. Phys. J. ST **228**(2), 261–623 (2019). <https://doi.org/10.1140/epjst/e2019-900045-4>
2. K. Oide, M. Aiba, S. Aumon, M. Benedikt, A. Blondel, A. Bogomyagkov, M. Boscolo, H. Burkhardt, Y. Cai, A. Dohlhammer et al., Phys. Rev. Accel. Beams **19**(11), 111005 (2016). <https://doi.org/10.1103/PhysRevAccelBeams.19.111005>
3. K. Oide, M. Benedikt, A. Blondel, A. Bogomyagkov, M. Boscolo, H. Burkhardt, B. Holzer, M. Koratzinos, E. Levicev, A. Milanese, et al. Proc. of Jacow-IPAC17-TUOCB1. <https://doi.org/10.18429/JACoW-IPAC2017-TUOCB1>
4. K. Oide, ICFA Beam Dyn. Newslett. **72**, 19–25 (2017)
5. P. Raimondi, D. Shatilov, M. Zobov, [arXiv:physics/0702033](https://arxiv.org/abs/physics/0702033) [physics]
6. M. Koratzinos, in Proc. 58th ICFA Advanced Beam Dynamics Workshop on High Luminosity Circular e^+e^- Colliders (eeFACT2016). <https://doi.org/10.18429/JACoW-eeFACT2016-TUT1AH3>
7. G. von Holtey et al., Study of beam induced particle backgrounds at the LEP detectors. Nucl. Instrum. Meth. A **403**, 205 (1998)
8. A. Novokhatski, M. Sullivan, E. Belli, M. Gil Costa, R. Kersevan, Phys. Rev. Accel. Beams **20**, 111005 (2017). <https://doi.org/10.1103/PhysRevAccelBeams.20.111005>
9. A. Novokhatski, Presented at the FCC WEEK (2020)
10. M. Boscolo, N. Bacchetta, M. Benedikt, L. Brunetti, H. Burkhardt, A. Ciarma, M. Dam, F. Franesini, M. Jones, R. Kersevan, et al., in Proc. of Jacow-IPAC21-WEPAB029 [arXiv:2105.09698 [physics.acc-ph]]
11. M. Boscolo, O. R. Blanco-Garcia, N. Bacchetta, E. Belli, M. Benedikt, H. Burkhardt, M. Gil Costa, K. Elsener, E. Leogrande, P. Janot, et al., Proc. of The 62nd ICFA advanced beam dynamics workshop on High luminosity circular $e+ecolliders$ (eeFACT2018), Jacow-eeFACT2018-WEXBA02. <https://doi.org/10.18429/JACoW-eeFACT2018-WEXBA02>
12. M. Boscolo, M.K. Sullivan, ICFA Beam Dyn. Newslett. **72**, 70–77 (2017)
13. M. Boscolo, H. Burkhardt, M. Sullivan, Phys. Rev. Accel. Beams **20**(1), 011008 (2017). <https://doi.org/10.1103/PhysRevAccelBeams.20.011008>

14. G. Voutsinas, K. Elsener, P. Janot, D. El Khechen, A. Kolano, E. Leogrande, E.F. Perez, N.A. Tehrani, O. Viazlo, M. Boscolo et al., FCC-ee interaction region backgrounds. *Int. J. Mod. Phys. A* **35**(15n16), 2041009 (2020). <https://doi.org/10.1142/S0217751X20410092>
15. M. Lückhof. PhD, thesis, Hamburg university, January 2021
16. M. Boscolo, O. Blanco-García, H. Burkhardt, F. Collamati, R. Kersevan, M. Lueckhof, *J. Phys. Conf. Ser.* **1067** (2018) no.2, 022012 <https://doi.org/10.18429/JACoW-IPAC2018-MOPMF085>
17. A. Ciarna, Presented at the FCC WEEK (2020)
18. H. Burkhardt, Presented at the FCC WEEK (2019)
19. K. Oide, Presented at the 3rd MDI workshop, CERN, September 2019